

See discussions, stats, and author profiles for this publication at: <https://www.researchgate.net/publication/255688341>

Reaction of Water with (Radicals in) Plasma Polymerized Allyl Alcohol (and Formation of OH-Rich Polymer Layers)

ARTICLE in THE JOURNAL OF PHYSICAL CHEMISTRY B · AUGUST 2013

Impact Factor: 3.3 · DOI: 10.1021/jp406186x · Source: PubMed

CITATIONS

5

READS

42

3 AUTHORS:



Alaa Fahmy

Al-Azhar University

21 PUBLICATIONS 56 CITATIONS

SEE PROFILE



A. Schönhals

Bundesanstalt für Materialforschung und -prü...

187 PUBLICATIONS 3,590 CITATIONS

SEE PROFILE



Jörg F. Friedrich

Technische Universität Berlin

203 PUBLICATIONS 2,208 CITATIONS

SEE PROFILE

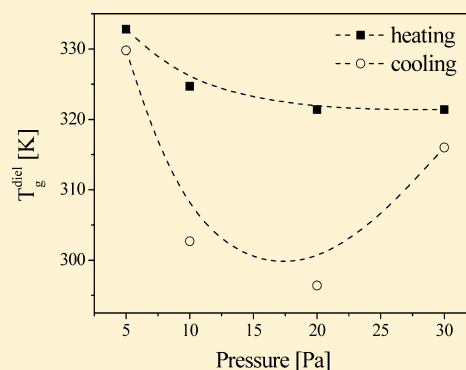
Reaction of Water with (Radicals in) Plasma Polymerized Allyl Alcohol (and Formation of OH-Rich Polymer Layers)

Alaa Fahmy,^{*,†,‡} Andreas Schönhals,[†] and Jörg Friedrich[†]

[†]BAM Federal Institute for Materials Research and Testing, Unter den Eichen 87, D-12205 Berlin, Germany

[‡]Chemistry Department, Faculty of Science, Al Azhar University, Nasr City, 11884 Cairo, Egypt

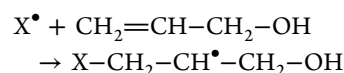
ABSTRACT: The pulsed plasma polymerization of allyl alcohol was employed under the aspect of maximal retention of OH groups and the formation of a regular polymer structure. It should be noted that earlier investigations on plasma polymers deposited from allyl alcohol did not show extensive postplasma addition of oxygen and water vapor from ambient air during storage, measuring the elemental O/C ratio by means of X-ray photoelectron spectroscopy (XPS). The identification of OH groups in the plasma polymerized polymer using FTIR spectroscopy was such an indicator for fragmentation. The peak area of OH groups in the film which was stored was increased by about 20% compared to that measured ("in situ"). These phenomenons reflected that moisture and O₂ in air played an important role in scavenging the free radicals. The addition of water and more specifically chemical bonding of OH of water in the deposited plasma polymer may serve as an indicator for monomer fragmentation, poly recombination, and the remaining radicals responsible for film formation. Moreover, the dielectric measurements show that the plasma deposited films are not thermally stable but undergo a postplasma chemical reaction during heating, where the reaction kinetics depends on pressure.



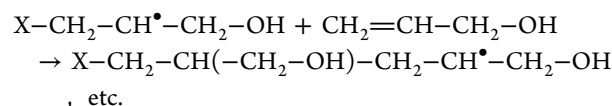
INTRODUCTION

Much attention has been paid in past decades to tailoring a polymer surface with special properties different from the bulk ones.^{1–4} Polymeric materials offer a variety of properties in the bulk; thus numerous applications in nearly every area of life are possible.⁵ Besides the bulk properties, the surface behavior of any material has a fundamental implication for its success in specific applications, as most of the interactions of a material take place through its common interface with the environment. Therefore, the advantageous bulk properties must be transferred versus the surface or interface to other materials or components as in composites. Often a particular polymer with desired bulk properties, such as polyolefins or fluoropolymers, possesses inappropriate surface properties, which consequently lead to adverse problems in adhesion, coating, painting, coloring, biocompatibility, etc. Several suggestions were explored to overcome such problems.⁶ One of them is the modification of a polymer surface for instance by plasma polymerization.

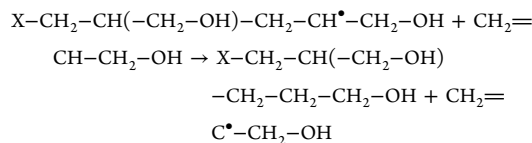
The radical polymerization of allyl alcohol (AAl) is distinctively different from the polymerization of vinyl monomers due to the chain transfer to the monomer according to



and



The side reaction is



The radicals formed by hydrogen abstraction are resonance stabilized, and frequently this results in termination because of the inability to start a chain. Therefore, the polymerization of allyl monomers leads to low molecular weight products.^{7–9}

Fally et al.¹⁰ studied plasma deposited PAAl films by X-ray photoelectron spectroscopy (XPS) and high resolution electron energy loss spectroscopy. They concluded that oxygen-rich polymers can be obtained from the unsaturated monomers at a low power. At high power, fragmentation of the monomer results in the elimination of oxygen fragments and in ablation

Received: April 23, 2013

Revised: August 6, 2013

Published: August 6, 2013



reactions as reported by Fahmy et al.⁴ The effect of the duty cycle was studied for thin plasma poly(allyl alcohol) films by a combination of dielectric spectroscopy, XPS, and Fourier transform infrared spectroscopy (FTIR).¹¹ As a result, the formation of polymers with a relatively low degree of cross-linking and high hydroxyl content (53–72%¹⁰) takes place under soft plasma conditions.

The goal in this field of plasma polymerization is to determine the structure–property relationships of plasma deposited poly(allyl alcohol) using advanced characterization methods. In particular, the retention ratios of OH groups in the allyl alcohol molecule and those in the plasma polymer were investigated. In this work the surface functionalization and volume properties of thin poly(allyl alcohol) plasma deposited films were investigated by a combination of dielectric relaxation spectroscopy, XPS, and FTIR where the monomer pressure was varied.

As discussed in our previous work,¹¹ during the plasma deposition of polymer films a highly branched product with many free radicals is formed. Carbonyl, carboxylate, and epoxy groups were also detected in addition to the hydroxyl groups in plasma poly(allyl alcohol) deposited films. As might be expected, the moisture and O₂ in air played an important role in scavenging the free radicals and the amount of OH groups in the film which was stored. Therefore, a systematic study of films after dipping in H₂O as a function of time was presented. This included also the investigation of postplasma reaction of the plasma polymer.

■ EXPERIMENTAL SECTION

Materials. Polyethylene (PE), polypropylene (PP), glass, and aluminum (Al) evaporated onto glass were used as substrates. The polyethylene (thickness 40 μm) and polypropylene (thickness 0.1 mm) foils were supplied by Alkor Folien GmbH, Germany. As the glass substrate, carefully cleaned (see below) microscope slides were used. Al was obtained from Goodfellow with a purity of 99.95%. Allyl alcohol (CH₂=CHCH₂OH, 99% purity), trifluoroacetic anhydride (99.5% purity), and deuterium oxide (D₂O, 99.95% purity) were obtained from MERCK (Germany).

Plasma Polymerization. The deposition experiments were accomplished in a stainless steel reactor (Ilmvac, Germany) of 50 dm³ volume. The reactor was equipped with a radio frequency (rf; 13.56 MHz) pulse generator with an automatic matching unit and a plain rf powered electrode (5 \times 35 cm). A stainless steel cylinder with a diameter of 10 cm served as a rotating grounded electrode. It was mounted at a distance of 2.5 cm with respect to the hot electrode. The rotation velocity of the cylinder was adjusted to 12 rpm. The monomer was dosed by a mass flow controller for liquids (Liqui-Flow, Bronkhorst) adjusted to 10 g/h and was introduced by a heatable gas/liquid distributor consisting of perforated metallic tubes. The pressure was kept constant during the process by varying the speed of the turbomolecular pump and adjusting an automatic butterfly valve (V.A.T.). A quartz microbalance was employed controlling the deposition rate where a 150 nm thick layer was deposited. Additionally, each sample was scratched and the thickness was measured by atomic force microscopy (AFM). A more detailed illustration about the apparatus has been given in a previous publication.¹¹

AAI was plasma polymerized using a duty cycle (DC = $t_{\text{on}}/(t_{\text{on}} + t_{\text{off}})$) of 0.5 and a pulse frequency of 1 kHz at an input power of 100 W. Therefore the effective power was 50 W.

Different samples were prepared by varying the process pressure with values of 5, 10, 20, and 30 Pa.

Influence of H₂O on the Stability of the Films. The samples deposited onto Al substrates were immersed in 60 mL of ultrahigh purity water (Millipore, resistivity > 18 M Ω /cm) for different times; after that they were dried in a dry nitrogen flow and analyzed by attenuated total reflection infrared spectroscopy (ATR-IR).

X-ray Photoelectron Spectroscopy (XPS). The surface composition and the functionality of PAAI were investigated by XPS (elemental composition) analyzing the C 1s peak. The employed spectrometer was a SAGE 150 (Specs, Berlin, Germany) equipped with a hemispherical analyzer (Phoibos 100 MCD-5). Nonmonochromatic Mg K α radiation with 11 kV and 220 W settings was used at a pressure of ca. 1×10^{-7} Pa in the analysis chamber. For more details see ref 11.

Derivatization of Functional Groups. The concentration of OH groups at the surface of deposited PAAI layers was quantified employing a derivatization with trifluoroacetic anhydride (TFAA) and subsequent XPS measurements.¹²

The reaction with TFAA converts OH groups into trifluoroacetates at the surface.¹¹ Using the fluorine signal in the XPS spectra, a quantification of the amount of OH groups is possible.

The plasma polymerized samples were exposed to a saturated TFAA vapor for 15 min, rinsed with isopropyl ether after that treatment extensively, and dried under vacuum prior to the XPS measurement as described elsewhere.¹¹

FTIR Spectroscopy. FTIR spectra were recorded in the wavenumber range from 4000 to 500 cm⁻¹ accumulating 64 scans with a resolution of 4 cm⁻¹ using a Nicolet Nexus 8700 FTIR spectrometer (Nicolet, USA) equipped with the appropriate ATR accessory (Diamond Golden Gate, one reflection, Nicolet, USA). All spectra were subjected to diamond ATR and baseline correction. In addition to estimating the peak areas by applying the OMNIC software, the spectra were analyzed by fitting Gaussians to the data.

Dielectric Spectroscopy. Broadband dielectric spectroscopy (BDS) was applied to investigate the molecular mobility of the prepared plasma polymerized layers. This method is sensitive to molecular fluctuations of dipoles within the system. For polymers these fluctuations are related to the molecular mobility of groups, segments, or the whole polymer chain as well; for more details see ref 13. Also the drift motion of charge carriers can be investigated. A high resolution alpha analyzer (Novocontrol) is used to measure the complex dielectric function $\epsilon^*(f) = \epsilon'(f) - i\epsilon''(f)$ (f , frequency; ϵ' and ϵ'' , real and imaginary parts of the complex dielectric function; $i = \sqrt{-1}$) in a frequency range from 10⁻¹ to 10⁷ Hz. The temperature of the sample was controlled by a Quatro Novocontrol cryo system with temperature stability better than 0.1 K. For more details see ref 14. For dielectric investigations the samples must be electrically contacted. Therefore, the polymer was prepared between two thin aluminum electrodes as described in ref 4 and given in Figure 1. The crossing area of the electrodes defines the capacitor for the measurement.

■ RESULTS AND DISCUSSION

Deposition Rate of Poly(allyl alcohol). The inset of Figure 2 displays thicknesses of the deposited layers versus deposition time for the different values of pressure. For each value of pressure, the data can be described by a straight line.

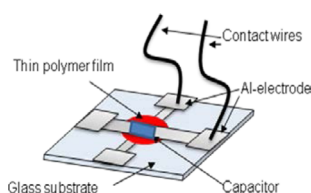


Figure 1. Sample capacitor for dielectric spectroscopy.

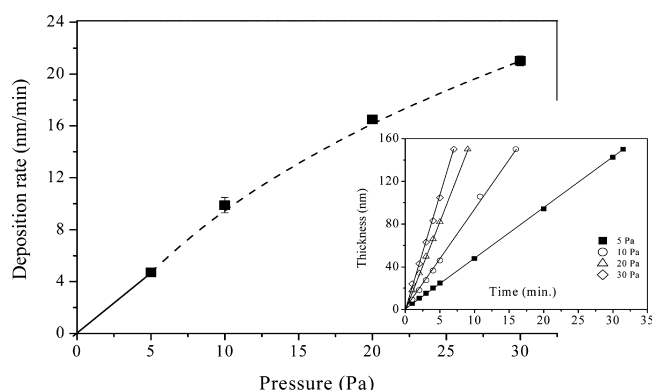


Figure 2. Deposition rate versus pressure (Pa). The error of the data is almost smaller than the size of the symbols. The inset gives the thickness of the plasma polymerized layer versus deposition time for various pressures. The lines are linear regressions to the corresponding data.

From its slope the deposition rate is obtained. With increasing pressure, the deposition rate increases for low values of pressure, but for higher values the deposition rate is slightly increased (see Figure 2). This means that the dependence of deposition rate versus pressure (Pa) is not linear as might be expected.

The idea of pressure pulsing is to establish a high concentration of monomer molecules in the plasma-off period of the pulsed plasma polymerization. In this plasma-off time, only chemically (radical) chain propagation occurs.⁴ The chain propagation process is strongly enhanced by increasing the monomer concentration and simultaneously the following chain terminating processes.

The additional pressure increases the sticking rate of monomer molecules at the chain propagation centers, thus

enhancing the chain propagation. Therefore, it also avoids early termination of the chain propagation reactions. If such a center does not find sufficient supply of monomers, then the stabilization of the energy-rich state by recombination, chain transfer, and disproportionation becomes dominating. In this case, only the next plasma pulse can reinitiate the chain propagation and the growing of the polymer chain. This way, the growing polymer layer is more or less chemically produced in the plasma-off period. After pumping down to low pressure, the reignition of plasma is possible and needs only low power input (Figure 2). At high pressure, the reignition of plasma is difficult and needs much more power input associated with thermal effects and additional monomer fragmentation. Nevertheless, these plasma pulses generally introduce irregularities into the polymer layer and produce byproducts in the case of the simple pulsed mode, as well as in the case of the pressure and plasma pulsed mode.¹⁵

Surface Functionalization. Figure 3 depicts the C 1s spectra of the deposited PAAl film before and after derivatization with TFAA of a sample prepared at a monomer pressure of 30 Pa as an example. The deconvolution of the C 1s peak of PAAl (Figure 3a) was performed assuming four components assigned to the following bonds: C–C/C–H, 285.0 eV; C–O, 286.3 eV; C=O, 287.5 eV; and COO, 289.1 eV. The corresponding fractions of the different components were estimated by fitting Gaussians to the data (cf. Figure 3).

As discussed above, C=O and COO groups were also detected in the plasma poly(allyl alcohol) deposited films (cf. Table 1). The fragmentation of the monomer and poly

Table 1. Surface Composition of Plasma Deposited PAAl Films at Different Pressures, As Determined by XPS

press. (Pa)	atomic composition (%)		ratio	C 1s deconvolution (%)			
				285 eV	286.3 eV	287.5 eV	289.1 eV
	C	O	O/C	C–C/C–H	C–O	C=O	O=C–O
5	78.2	21.8	0.28	59.1	31.2	08.5	1.2
10	76.8	23.1	0.30	58.1	26.4	12.8	2.7
20	77.6	22.4	0.29	62.4	20.9	14.6	2.1
30	81.7	18.2	0.22	69.1	15.6	12.8	2.5

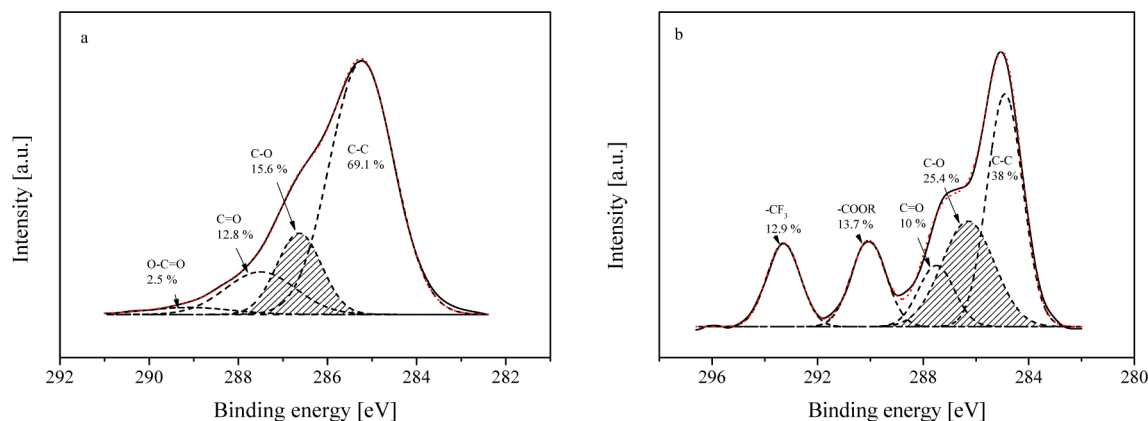
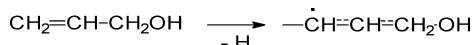


Figure 3. Set of C 1s peaks of the PAAl sample prepared at 30 Pa (a) before derivatization and (b) after derivatization with TFAA. The solid line represents the experimental data. The dotted line is a fit of a sum of four or five Gaussians to the data. The dashed lines represent the individual contributions.

recombination followed by postplasma oxidation as well are the reason for formation of these groups. In addition to radical polymerization (regular structure) of poly(allyl alcohol), hydrogen abstraction might have occurred and allylic radicals were formed. In the presence of allylic radicals have enol resonance structures as given here,



which can tautomerize to aldehyde or simple fragmentation and a formation of $>\text{C}=\text{O}$ structures by recombination occurs.

The allylic radicals formed in the abstraction reaction are relatively unreactive to other allyl monomers because of their resonance stabilization and thus lead to termination.^{16,7}

The C 1s spectrum of the derivatized samples at different pressures was deconvoluted into five peaks, including an additional component at 293.0 eV corresponding to the CF_3 bond. Following the derivatization reaction equal intensity for three peaks must be employed: one for $-\text{CF}_3$, one for $\text{O}=\text{C}-\text{O}-$, and that for $\text{O}=\text{C}-\text{O}-\text{CR}$. The intensity of the last one is the highest. This means that some C–O bonds have to be assigned to ether-type linkages, which do not participate in the derivatization reaction and remain therefore unchanged.

From these data the concentration of hydroxyl groups per 100 carbon atoms $C_{(\text{OH})}$ can be calculated by

$$C_{(\text{OH})} = 100 \frac{[\text{F}]}{3[\text{C}] - 2[\text{F}]} \quad (1)$$

where the concentrations of carbon [C] and fluorine [F] were estimated from the XPS spectra of the derivatized sample.¹¹ $C_{(\text{OH})}$ is plotted versus the monomer pressure in Figure 4.

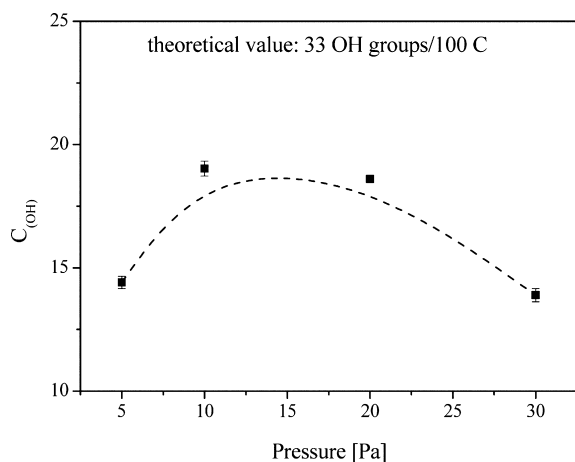


Figure 4. Concentration of hydroxyl groups per 100 carbon atoms versus monomer pressure. The error bars results from three different measurements at the same sample. Theoretical values of OH groups equal 33 per 100 C atoms, indicates the maximal possible concentration of hydroxyl groups.

First, the concentration of hydroxyl groups is much smaller than the value expected from the regular chemical structure of poly(allyl alcohol) and which was found recently with maximal 30% OH/C.¹⁷ This effect is related to the different amounts of monomer fragmentation due to the particular plasma conditions. The fragmentation and rearrangement of the monomer result in a lower concentration of hydroxyl groups and a higher concentration of radicals.¹⁸ Second, $C_{(\text{OH})}$ increases up to a monomer pressure of ca. 10 Pa and decreases

after the maximum with increasing pressure. Variations of the reaction pressure lead to several effects which take place simultaneously. For instance, when the reaction pressure is increased, the mean free path of the plasma particles decreases. This leads to an increase in the collision rate, and therefore, the fragmentation and rearrangement of the monomer molecules will increase. However, when the mean free path of the electrons decreases, they gain less energy from the electric field and their collision rate with the neutral molecules increases, too. These results in a decrease in electron temperature (T_e), which should decrease the fragmentation and rearrangement of the monomer molecules.¹⁹ Therefore, the found pressure dependence of $C_{(\text{OH})}$ results from a counterbalance of these two effects. For low pressure at 5 Pa, the first process wins, while the second process is preferable for higher pressures in the range from 7 to 25 Pa. For higher pressure than 20 Pa plasma poly(allyl alcohol) is deposited as a high viscous liquid. It should be noted that the energy coupling into the plasma is also influenced because of changes in the resonant circuit by different values of the Ohmic resistance, the capacity, and the inductivity by varying the pressure in the plasma. The other observation is that the ratio of O/C varying similar to $C_{(\text{OH})}$ is obtained while the concentration of C–O bonds decreases with increasing pressure (cf. Table 1).

The concentration of C–O groups (includes C–O–C and C–O–H groups) decreases with increasing pressure. The reason for that behavior is the oxygen might be also incorporated into the plasma deposited films from two further sources. First, the used reactor is not a ultrahigh vacuum reactor, and has a low but unavoidable leak rate. Thus, a certain amount of oxygen may become incorporated into the plasma deposited film through background leakage of oxygen into the reactor or from residual oxygen in the reactor. The oxygen concentration from such sources would be expected to decrease with increasing deposition pressure, which it does, as is reflected by the decreasing O/C ratio in the XPS spectrum as deposition pressure is increased.

Second, oxygen may be incorporated if the film is exposed to the air upon removal from the plasma reactor. Unreacted radical species in the plasma deposited film may react with oxygen or water vapor in the air, which can be seen by increasing oxygen concentrations in the plasma polymer during storage.

Investigation of PAAL Films by ATR-IR. In this section, PE and PP as organic substrates and aluminum and glass as inorganic substrates were used.

The successful surface functionalization is also evident from ATR-IR analysis as depicted in Figure 5, which shows the FTIR spectra of PAAL deposited on an Al substrate for different values of the monomer pressure as an example. Besides, the peaks characteristic for the substrates exhibit the stretching vibrations which are characteristic for poly(allyl alcohol): the $\nu(\text{OH})$ stretching vibration at $\sim 3400 \text{ cm}^{-1}$ associated with $\nu(\text{CH}_3^{\text{as}})$ at $\sim 2940 \text{ cm}^{-1}$, $\nu(\text{CH}_2^{\text{as}})$ at $\sim 2920 \text{ cm}^{-1}$, $\nu(\text{CH}_3^{\text{s}})$ at $\sim 2890 \text{ cm}^{-1}$, and the $\nu(\text{CH}_2^{\text{s}})$ vibrations at $\sim 2880 \text{ cm}^{-1}$ are observed together with the corresponding $\nu(\text{C}-\text{O})$ vibration at $\sim 1047 \text{ cm}^{-1}$.²⁰

After the abstraction of the allylic hydrogen by radicals, chain ends with vinyl groups and aldehyde groups can be obtained.⁷ Therefore, the $\text{C}=\text{O}$ stretching vibration characteristic for carbonyl bonds near 1700 cm^{-1} is also found. Therefore, in addition to the XPS investigations the FTIR investigations show the deposition of PAAL. However, the most important

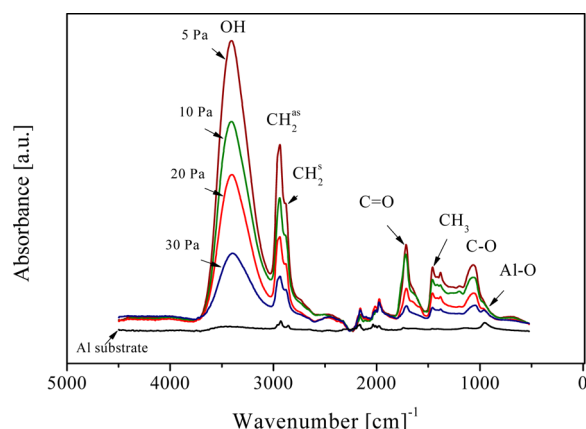


Figure 5. FTIR spectra of PAAL deposited on Al for different values of the monomer pressure in comparison to Al substrate as a blank.

peak for the following discussion is the stretching vibration of hydroxyl groups (OH).

From fits the areas of the Gaussians at ~ 3300 (A_{OH}) and ~ 2890 cm^{-1} ($A_{\text{CH}_3(\text{s})}$) are taken and their ratio $A_{\text{OH}}/A_{\text{CH}_3}$ is calculated as a measure for the concentration of OH groups estimated from FTIR. The reference to the CH_3 vibration is an approximation which is only exactly valid if the concentration of the CH_3 groups does not depend on the pressure due to fragmentation and at a constant value of W/FM.¹¹

Figure 6a shows the enlarged view in the wavenumber range of the OH vibration from ca. 3650 to 3050 cm^{-1} for PAAL. A detailed examination reveals that this band consists at least of two different contributions. The main component at ~ 3300 cm^{-1} is attributed to the hydroxyl stretching vibration (C–OH) of PAAL. The second contribution with a shoulder at ~ 3450 cm^{-1} is related to the vibration of another structural unit. According to the literature, this band is due to hydrogen bonded H–OH or OH groups from peroxy which may be formed due to fragmentation of the monomer and poly recombination or oxygen incorporation.²¹ For quantitative analysis two Gaussians are fitted to the data.

The peak area of the $\nu(\text{OH})$ stretching vibration at ~ 3300 cm^{-1} referenced that of the $\nu(\text{CH}_3^{\text{s}})$ vibration at ~ 2890 cm^{-1} . The peak area of the $\nu(\text{OH})$ vibration increases with pressure for low pressures, and then it starts to decrease from 20 Pa as the partial pressure of PAAL in the reaction mixture is increased further (cf. Figure 7).

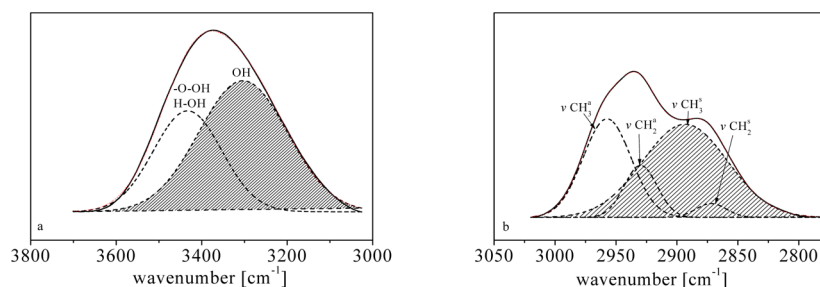


Figure 6. (a) Wavenumber region for the hydroxyl groups and (b) for both the asymmetric and symmetric $-\text{CH}_2$ and $-\text{CH}_3$ stretching vibrations of PAAL deposited on aluminum substrate at pressure = 10 Pa as an example. The spectra are analyzed by fitting two and four Gaussians to the data for hydroxyl group and (asymmetric and symmetric $-\text{CH}_2$ and $-\text{CH}_3$), respectively. The solid line represents the experimental data. The dotted line is a fit of a sum of four Gaussians to the data. The dashed lines represent the individual contributions. The inset gives the high resolution XPS spectra of pure PE.

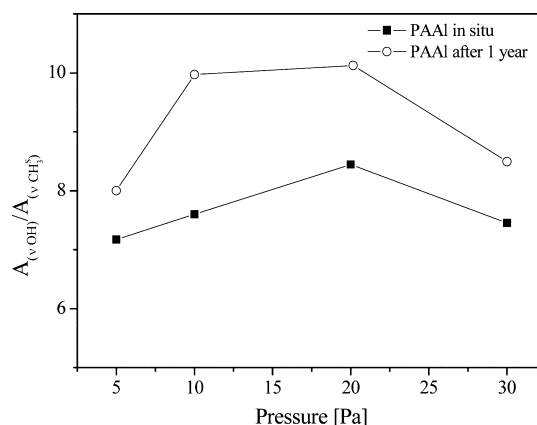


Figure 7. Concentration of OH groups as estimated by $A_{\nu(\text{OH})}/A_{\nu(\text{CH}_3)}$ versus monomer pressure: in situ (without storage) and after 1 year storage for films deposited on Al substrate.

Influence of the Storage Time on the Structure of Films. All plasma deposited films were examined after 1 year annealing in air. Discussion of the dependence of deposition rates on pressure shows a substantial increase of the amount of additional oxygen compared to the prepared sample (in situ). The increase of the concentration of OH groups with increasing storage time indicates that active free radicals were quenched by molecular oxygen and subsequent autoxidation during aging under atmospheric pressure and room temperature takes place. Oxygen and moisture in the air can combine with free radicals and thus act as their scavenger, leading to decay in free radical concentration, and therefore, the concentration of OH groups is increased.²²

The amount of OH groups in the film which was stored was increased by about 20% compared to that measured (“in situ”). These phenomena reflected that moisture and O_2 in air played an important role in scavenging the free radicals as discussed before and in agreement with the literature (cf. Figure 7).²³

Independent of the incorporation of oxygen under formation of peroxy groups and subsequent autoxidation, the influence of water on the aging process of PAAL should be investigated. Therefore, a systematic study of the PAAL structure as a function of the exposure of films to ultrahigh purified water (Millipore, resistivity > 18 $\text{M}\Omega/\text{cm}$ [deionized water]) for different times was carried out.

Influence of the Storage of Plasma Polymerized Poly(allyl alcohol) Films in Deionized Water (D H₂O) on Structure and Composition. The samples of PAAI were exposed to deionized water for several hours at room temperature. After the samples were allowed to dry, the FTIR spectra did not indicate permeation of water to any detectable extent into the surface region. Thus moisture adsorption during sample transfer, sample aging effects, etc., can be eliminated from contributing to the infrared results in Figure 8.

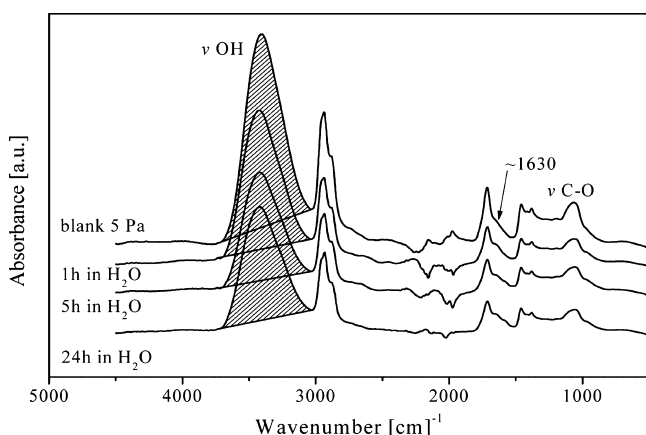


Figure 8. FTIR spectra of PAAI deposited on Al for PAAI polymerized at 5 Pa and rinsed in deionized H₂O for different times compared to the original sample as blank.

It should be noted that the deposited poly(allyl alcohol) can be dissolved and may be a dissolution of low molecular weight. Therefore, some of OH groups were removed by this process, leading to decrease of the intensity of spectra after prolonged immersion in water and, therefore, the hydrogen bond (cf. Figure 8).²⁴

Otherwise, the concentration of OH groups was increased during the first 5 h in water at all pressures and then it decreased with increasing dipping time. This indicates that the free radical decay is accelerated by the exposure to water and leads to the formation of a OH-rich layer (cf. Figure 9). Besides, with further dipping time than 5 h, the intensity of the spectrum starts to decrease due to the partial removal of films as discussed above.

To ensure that the changes in the spectrum are due to plasma effects alone, samples of PAAI were placed in D₂O at the same condition as that used for deionized H₂O. The exchange was quite rapid; the samples were permitted to remain in D₂O for 1 h at room temperature.

There are two indications: first the intensity of the spectrum decreases at all wavenumbers below that of the reference spectrum of the control sample and that rinsed in water. PAAI could readily interact with D₂O and showed a pronounced shift of approximately 900 cm⁻¹ (from ~3400 to ~2600 cm⁻¹). This shift is common for -OD versus -OH adsorption and indicates that the exchange process takes place between hydroxyl and deuterioxyl groups. For more than 1 h in D₂O, the spectrum of the aluminum substrate only is observed without any indication for PAAI layers. Second, the maximum position of hydroxyl groups shows pronounced shifts of approximately 20 cm⁻¹ for samples of PAAI placed in D₂O

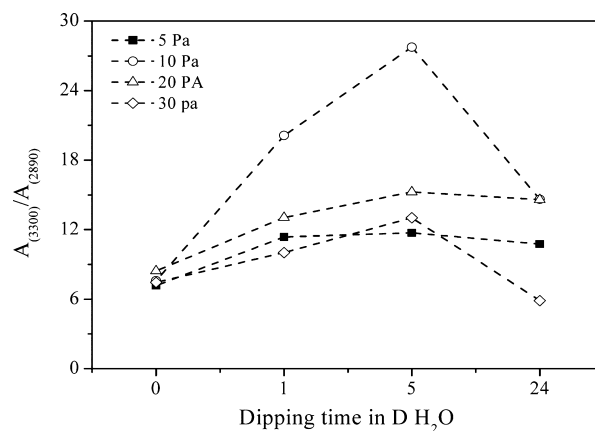


Figure 9. Concentration of OH groups as estimated by $A_{\nu(\text{OH})}/A_{\nu(\text{CH}_3)}$ versus dipping time in deionized H₂O for different monomer pressures.

and H₂O in comparison to the control sample (cf. Figure 10). This shift is common for -OD and -OH adsorption.²³

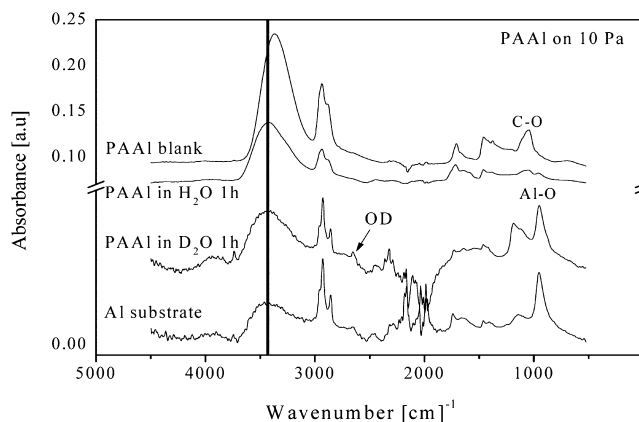


Figure 10. FTIR spectra of PAAI deposited on Al substrate at 10 Pa rinsed in deionized H₂O and D₂O for 1 h and compared to the original sample as blank.

Effect of the Substrate on the Structure of Films. A closer inspection of the OH stretching vibration shows that the maximum peak position is shifted to a higher wavenumber by ca. 20 cm⁻¹ in the cases of PE, PP, and glass substrates in comparison to that of the liquid allyl alcohol monomer. The reason is the plasma energy not only attacks the monomer vapor but also attacks the surfaces of substrates in the beginning of the deposition process. Therefore, some radicals and oxygen groups (hydroxyl, carbonyl, ether, and epoxy groups) might be generated on the substrates. At the same time hydrogen bonds can be formed between hydroxyl groups of PAAI and the new functional groups were created on the substrate surface leading to the shift of the OH vibration to higher wavenumbers.

In the case of the glass substrate, its surface carries hydroxyl (silanol) groups, which can form also hydrogen bonds to the alcoholic OH groups of the PAAI in a similar way as found for polymer substrates.

The peak position of hydroxyl groups is shifted to essentially higher wavenumbers (50 cm⁻¹) compared to that of the liquid monomer in the case of the Al substrate. In this case, the large shift is probably due to the lone pair of electrons of oxygen of the OH group. It can react with Al and form a coordination

bond¹¹ (cf. Table 2). A similar behavior is observed for all other values of the monomer pressure.

Table 2. Position of the Maximum of $\nu(\text{OH})$ Stretching Vibration for Plasma Deposited PAAI on Different Substrates at 30 Pa as an Example

substrate	wavenumber (cm^{-1}) at max band of $\nu(\text{OH})$ vibr
polyethylene (PE)	3358
polypropylene (PP)	3368
glass	3369
aluminum (Al)	3392
allyl alcohol (blank)	3341

Dynamic Mobility and Thermal Stability. To investigate the molecular dynamics of thin polymer films, dielectric spectroscopy (BDS) as a probe for their structure is employed. It was proven that BDS is a powerful tool to investigate the molecular mobility and the conductivity which both are related to the structure of polymers.²⁵

In the frame of the linear response theory real and imaginary (loss) parts of the complex dielectric function are related to each other by the Kramers–Kronig relationships. Therefore, both quantities contain the same information and here only ϵ'' (dielectric loss) is discussed. Figure 11 gives the dielectric loss

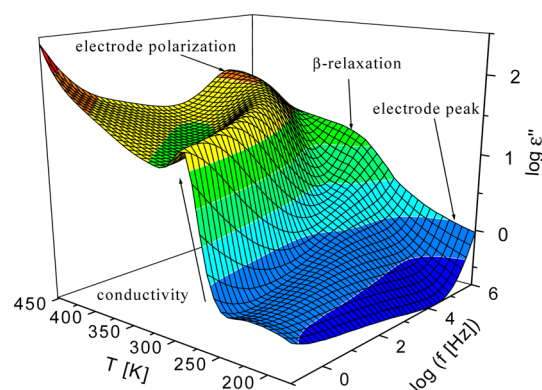


Figure 11. Dependence of dielectric loss ϵ'' versus frequency and temperature for PAAI at 20 Pa, recorded on the cooling cycle.

for PAAI at 20 Pa versus frequency and temperature in a three-dimensional representation during cooling from 450 to 150 K. A relaxation process indicated by a peak in the dielectric loss is observed at low temperature and is called β -relaxation. It corresponds to localized molecular fluctuations. As expected, the maximum position of the peak shifts to higher frequency with increasing temperature. At higher temperatures than those of the β -relaxation a second process is observed which is a huge dielectric intensity. No dipole in the system can explain this high dielectric strength. Therefore, it was assigned to electrode polarization. Electrode polarization is related to the drift motion of charge carriers, which are blocked at electrodes which do not behave completely ohmic. This causes an additional capacitance in the system which is permanently charged/discharged by the measuring electric ac field.

The resistance $R_{\text{Electrode}}$ of the evaporated Al electrodes cannot be neglected for the thin film capacitors considered here. This resistance leads to an artificial loss contribution (electrode peak) on the high-frequency side of the spectra with a time constant $\tau_{\text{Res}} = R_{\text{Electrode}} C'$ (C' , sample capacity). As the

resistance R of the Al electrodes does not change with temperature dramatically, the frequency position of the electrode peak is constant.

The Havriliak and Negami function (HN function) is used to analyze the data.²⁶ The electrode peak is taken into consideration by a Debye function taking into account its low frequency approximation as described in ref 13. Therefore, the whole fit function reads as

$$\epsilon''(f) = \text{Im} \left\{ \frac{\Delta\epsilon}{(1 + (if/f_0)^\beta)^\gamma} \right\} + Af \quad (2)$$

where A is a fitting parameter which is mainly due to τ_{Res} .

Electrode polarization is due to the blocking of charge carriers at the electrodes. In the considered experiments, aluminum is evaporated as electrodes which have also an oxide layer can block charge carriers. It is well-known that the blocking of the charge carriers at the electrodes can be described by an electrical double layer with an effective spacing characterized by its Debye length L_D . This double layer represents an additional capacitance C_{DL} in the system and the time dependence of the polarization is due to the charging/discharging of that electrical double layer. The time constant (τ_{EP}) for electrode polarization is related to the conductivity σ of the system. Although an interfacial polarization is not a relaxation process, it can be also analyzed by fitting the HN function to the data and the rate for electrode polarization $f_{\text{EP}} \sim 1/\tau_{\text{EP}} \sim 1/\text{s}$ can be estimated in its temperature dependence.

It is known that the mobility of polymer segments depends on the temperature.^{4,27}

The dependence of f_{EP} on temperature is curved when plotted versus $1/T$ and might be analyzed by the Vogel/Fulcher/Tammann (VFT) formula,²⁸ which reads

$$\log f_p = \log f_\infty - \frac{A}{T - T_0} \quad (3)$$

where $\log f_\infty$ and A are constants. T_0 is the so-called Vogel or ideal glass transition temperature.

Figure 12 compares the temperature dependence of the electrode polarization rate for the different values of the pressure on heating. First, with increasing pressure the rate of the electrode polarization shifts to lower values of the temperature. The conductivity which dominates f_{EP} is related to the segmental mobility which is responsible for glassy dynamics in polymeric systems. A crude estimation of a dielectric glass transition temperature can be estimated by $T_g^{\text{diel}} = T(f_{\text{EP}} = 1 \text{ Hz})$.

T_g^{diel} is plotted versus pressure of the monomer in the inset of Figure 12. As already seen from the raw data, with increasing monomer pressure from 5 to 20 Pa, T_g decreases and increases after a minimum with further increases of the monomer pressure. It is worth noting that the pressure dependence of the glass transition temperature is quite similar to the results found by XPS and FTIR (compare Figure 12 with Figures 3 and 5). This might mean that the cross-linking becomes weaker with increasing pressure from 7 to 25 Pa and the regular structure (growing of linear polymer chains) is growing.

The second run is the subsequent cooling from high to low temperatures. The estimated dependence of T_g on monomer pressure is like that observed for heating, but the values of T_g are lower than that for the heating process. Molecular translational and rotations at elevated temperature offered

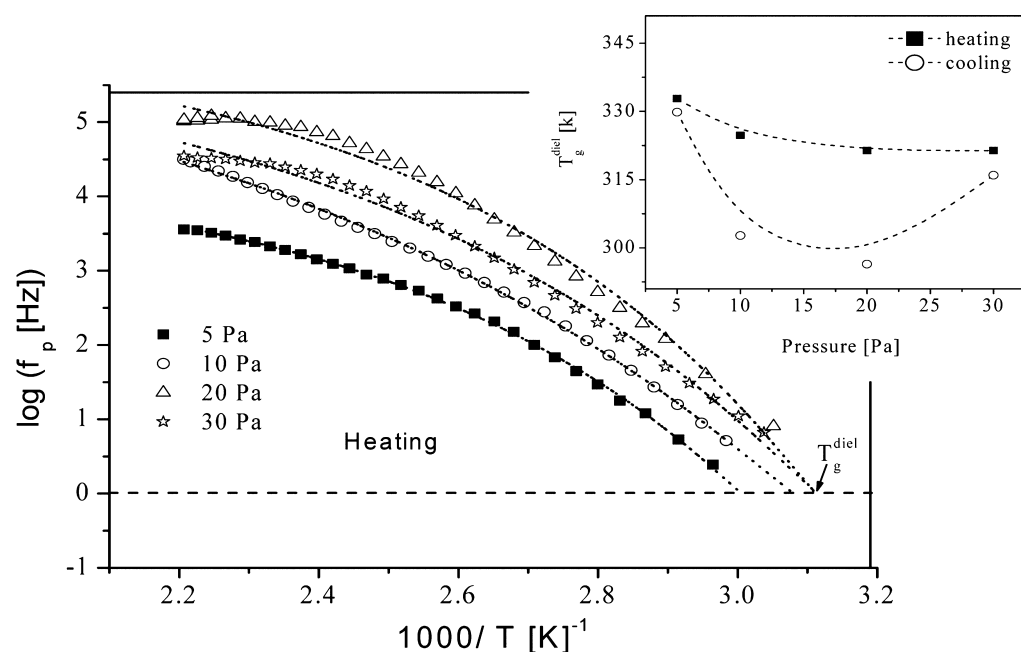


Figure 12. Relaxation rate of electrode polarization versus inverse temperature for plasma deposited PAAL for different pressures on heating. The inset shows the dynamic glass transition temperature T_g^{diel} versus pressure for different processes: heating and cooling.

more opportunities for the neighboring radicals to collide/meet and, thereby, provide the possibility for free radical recombination.^{11,29} As discussed in our previous work,^{4,11,26} during the plasma deposition of the polymer film a highly branched product with many free radicals is formed. To reveal the nature of this, further investigations are necessary which are under preparation. The decrease of the estimated glass transition temperature points to a dangling ends reaction.

CONCLUSIONS

Thin PAAL films were deposited by pulsed plasma polymerization on different substrates (organic and inorganic). The structure–property relationships of allyl alcohol polymers were studied in dependence on pressure (Pa) by various techniques and probes.

A derivatization technique in combination with XPS measurements was used to get information on the hydroxyl group concentration of the plasma deposited PAAL.

The concentration of hydroxyl groups is much smaller than the value expected from the regular chemical structure of poly(allyl alcohol). This effect is related to the different amounts of monomer fragmentation due to the particular plasma conditions. The fragmentation and rearrangement of the monomer result in a lower concentration of hydroxyl groups and a higher concentration of radicals.

FTIR-ATR measurements were carried out to calculate the OH concentrations quantitatively. During the plasma deposition of polymer films a highly branched product with many free radicals is formed. Carbonyl, carboxylate, and epoxy groups were also detected in addition to the hydroxyl groups in plasma poly(allyl alcohol) deposited films.

The moisture and O_2 in air played an important role in scavenging the free radicals and the amount of OH groups in the film which was stored was increased by about 20% compared to that measured (“in situ”). Additionally, the free radical decay is accelerated by the exposure to water and leads to the formation of OH groups.

The dielectric measurements reveal that the structure of the plasma deposited polymer is dependent on the pressure. The cross-linking becomes weaker with increasing pressure up to 20 Pa and the regular structure is favorable. Otherwise, the values of T_g are lower for the cooling process than for the heating one. Molecular translational and rotations at elevated temperature offered more opportunities for the neighboring radicals to collide/meet and, thereby, provide the possibility for free radical recombination.

AUTHOR INFORMATION

Corresponding Author

*Tel.: +49 30/8104-4658. Fax: +49 30/8104-1637. E-mail: a1_fahmy@yahoo.com.

Notes

The authors declare no competing financial interest.

REFERENCES

- (1) Sun, J.; Yao, L.; Sun, S.; Gao, Z. Q.; Qiu, Y. P. Effect of Storage Condition and Aging on Acrylic Acid Inverse Emulsion Surface-Grafting Polymerization of PET Films Initiated by Atmospheric Pressure Plasmas. *Surf. Coat. Technol.* **2011**, *205*, 2799–2805.
- (2) Biesalski, M.; Ruehe, J. Preparation and Characterization of a Polyelectrolyte Monolayer Covalently Attached to a Planar Solid Surface. *Macromolecules* **1999**, *32*, 2309–2316.
- (3) Lamb, D. J.; Anstey, F. C.; Fellows, M.; Monterio, M. J.; Gilbert, R. G. Modification of Natural and Artificial Polymer Colloids by “Topology-Controlled” Emulsion Polymerization. *Biomacromolecules* **2001**, *2*, 518–525.
- (4) Fahmy, A.; Mix, R.; Schönhals, A.; Friedrich, J. F. Structure of Plasma-Deposited Poly(acrylic acid) Films. *Plasma Processes Polym.* **2011**, *8*, 147–159.
- (5) Weinberg, B. D.; Blanc, E.; Ga, J. M. Polymer implants for intratumoral drug delivery and cancer therapy. *J. Pharm. Sci.* **2008**, *97*, 1681–1702.
- (6) Yameen, B.; Tamm, M.; Vogel, N.; Echler, A.; Förch, R.; Jonas, U.; Knoll, W. Cyanate Ester Resins as Thermally Stable Adhesives for Polyether Ether Ketone. In *Surface Design: Applications in Bioscience*

and Nanotechnology; Förch, R., Schönherr, H., Jenkins, A. T. A., Eds.; Wiley-VCH: Weinheim, Germany, 2009; p 145.

(7) Oh, S. J.; Kinney, D. R.; Wang, W.; Rinaldi, P. L. Studies of Allyl Alcohol Radical Polymerization by PFG-HMQC and HMBC NMR at 750 MHz. *Macromolecules* **2002**, *35*, 2602–2607.

(8) Guo, S. H. Allyl Alcohol- and Allyl Alkoxyate-Based Polymers. *Specialty Monomers and Polymers*; Havelka, K. O., McCormick, C. L., Eds.; ACS Symposium Series 755; American Chemical Society: Washington, DC, 2000; pp 147–158.

(9) Inoue, S.; Kumagai, T.; Tamezawa, H.; Aota, H.; Matsumoto, A.; Yokozama, K.; Matoba, Y.; Shibano, M. Pursuit of Reinitiation Efficiency of Resonance-Stabilized Monomeric Allyl Radical Generated via “Degradative Monomer Chain Transfer” in Allyl Polymerization. *J. Polym. Sci., Part A: Polym. Chem.* **2011**, *49*, 156–163.

(10) Fally, F.; Virlet, I.; Riga, J.; Verbist, J. J. Detailed Multitechnique Spectroscopic Surface and Bulk Characterization of Plasma Polymers Deposited from 1-Propanol, Allyl Alcohol, and Propargyl Alcohol. *J. Appl. Polym. Sci.* **1996**, *59*, 1569–1584.

(11) Fahmy, A.; Mix, R.; Schönhals, A.; Friedrich, J. F. Structure-Property Relationship of Thin Plasma Deposited Poly(allyl alcohol) Films. *Plasma Chem. Plasma Process.* **2011**, *31*, 477–498.

(12) Chilkoti, A.; Ratner, B. D. *Surface Characterization of Advanced Polymers*; Sabbattini, L., Zamboni, P. G., Eds.; Wiley-VCH: Weinheim, Germany, 1996; p 221.

(13) Schönhals, A. In *Broadband Dielectric Spectroscopy*; Kremer, F., Schönhals, A., Eds.; Springer: Berlin, 2002; p 225.

(14) Kremer, F.; Schönhals, A. In *Broadband Dielectric Spectroscopy*; Kremer, F., Schönhals, A., Eds.; Springer: Berlin, 2002; p 35.

(15) Friedrich, J. F.; Mix, R.; Schulze, R. D.; Meyer-Plath, A.; Joshi, R.; Wettmarshausen, S. New Plasma Techniques for Polymer Surface Modification with Monotype Functional Groups. *Plasma Processes Polym.* **2008**, *5*, 407–423.

(16) Watkins, L.; Bismarck, A.; Lee, A. F.; Wilson, D.; Wilson, K. An XPS Study of Pulsed Plasma Polymerised Allyl Alcohol Film Growth on Polyurethane. *Appl. Surf. Sci.* **2006**, *252*, 8203–8211.

(17) Friedrich, J.; Mix, R.; Kühn, G.; Retzko, I.; Schönhals, A.; Unger, W. Plasma-Based Introduction of Monosort Functional Groups of Different Type and Density onto Polymer Surfaces. Part 2: Pulsed Plasma Polymerization. *Compos. Interfaces* **2003**, *10*, 173–223. Friedrich, J.; Kühn, G.; Mix, R.; Unger, W. Formation of Plasma Polymer Layers with Functional Groups of Different Type and Density at Polymer Surfaces and their Interaction with Al Atoms. *Plasma Processes Polym.* **2004**, *1*, 28–50.

(18) Swaraj, S.; Oran, U.; Lippitz, A.; Friedrich, J. F.; Unger, W. E. S. Aging of Plasma-Deposited Films Prepared from Organic Monomers. *Plasma Processes Polym.* **2007**, *4*, S784–S789.

(19) Swaraj, S.; Oran, U.; Friedrich, J. F.; Lippitz, A.; Unger, W. E. S. Surface Analysis of Plasma-Deposited Polymer Films, 6. Analysis of Plasma Deposited Allyl Alcohol Films Before and After Aging in Air. *Plasma Processes Polym.* **2005**, *2*, 572–580.

(20) Del Fanti, N. A. *Infrared Spectroscopy of Polymers*; Thermo Fisher Scientific: Waltham, MA, USA, 2008.

(21) Nada, A. M. A.; Ibrahim, A. A.; Fahmy, Y.; Abo-Yousef, H. E. Peroxyacetic Acid Pulp of Bagasse and Characterization of the Lignin and Pulp. *J. Sci. Ind. Res.* **1999**, *58*, 620–628.

(22) Sabharwal, H. S.; Denes, F.; Nielsen, L.; Young, R. A. Free-Radical Formation in Jute from Argon Plasma Treatment. *J. Agric. Food Chem.* **1993**, *41*, 2202–2207.

(23) Memetea, T.; Stannett, V. Radiation Grafting to Poly(ethylene terephthalate) Fibres. *Polymer* **1979**, *20*, 465–468.

(24) Bruckner, R. In *Advanced Organic Chemistry*; Elsevier: Amsterdam, 2002.

(25) *Dielectric Spectroscopy of Polymeric Materials*; Runt, J. P., Fitzgerald, J. J., Eds.; American Chemical Society: Washington, DC, 1997.

(26) Schlosser, E.; Schönhals, A. Recent Development in Dielectric Relaxation Spectroscopy of Polymers. *Colloid Polym. Sci.* **1989**, *267*, 963–969.

(27) Larsen, M. J.; Ma, Y.; Qian, H.; Toftlund, H.; Lund, P. B.; Skou, E. M. Stability of Radicals in Electron-Irradiated Fluoropolymer Film for the Preparation of Graft Copolymer Fuel Cell Electrolyte Membranes. *Solid State Ionics* **2010**, *181*, 201–205.

(28) Fahmy, A.; Mix, R.; Schönhals, A.; Friedrich, J. Structure of Plasma-Deposited Copolymer Films Prepared from Acrylic Acid and Styrene: Part I Dependence on the Duty Cycle. *Plasma Processes Polym.* **2012**, *9*, 273–284.

(29) Mitov, S.; Hübner, G.; Brack, H.-P.; Scherer, G. G.; Roduner, E. In Situ Electron Spin Resonance Study of Styrene Grafting of Electron Irradiated Fluoropolymer Films for Fuel Cell Membranes. *J. Polym. Sci., Part B: Polym. Phys.* **2006**, *44*, 3323–3336.